

Bandgap and Molecular Energy Level Control of Conjugated Polymer Photovoltaic Materials Based on Benzo[1,2-*b*:4,5-*b'*]dithiophene

Jianhui Hou,* Mi-Hyae Park, Shaoqing Zhang, Yan Yao, Li-Min Chen, Juo-Hao Li, and Yang Yang*

Department of Materials Science and Engineering & California Nanosystems Institute, University of California, Los Angeles, Los Angeles, California 90095

Received April 13, 2008; Revised Manuscript Received June 13, 2008

ABSTRACT: Bandgap and molecular energy level control are of great importance in improving photovoltaic properties of conjugated polymers. A common approach to tuning these parameters is to modify the structure of conjugated polymers by copolymerizing with different units. In this paper, research work focuses on the synthesis of benzo[1,2-*b*:4,5-*b'*]dithiophene (BDT) with different conjugated units and their photovoltaic performance. Eight new BDT-based polymers with commonly used conjugated units, including thiophene, benzo[*c*][1,2,5]thiadiazole (BT), thieno[3,4-*b*]pyrazine (TPZ), etc., were synthesized. The bandgaps of the polymers were tuned in the range of 1.0–2.0 eV, and their HOMO and LUMO energy levels could also be tuned effectively. The absorption spectra as well as electrochemical and photovoltaic properties of these polymers were investigated systematically. Some units exhibiting the same effect of bandgap lowering exhibited different effects on molecular energy levels of the polymers. For example, the TPZ unit can reduce the bandgap by lowering the LUMO energy level and elevating the HOMO level of the polymer, but the BT unit can lower the bandgap only by depressing the LUMO level. Since open-circuit voltage (V_{oc}) of the heterojunction polymer solar cell is believed to be inversely proportional to the HOMO level of electron donor material, V_{oc} of the devices based on H9, the copolymer of BDT and TPZ, was ca. 0.5 V lower than that of the device based on H7, the copolymer of BDT and BT. The effects of seven commonly used units on bandgap, molecular energy level, and photovoltaic properties of the BDT based polymers are studied and discussed in this paper, which can provide a guideline not only for design of photovoltaic materials but also for materials of various other electronic devices. In addition, the PCE of the device based on PCBM and H6, one of the BDT-based polymers, reached 1.6%, and V_{oc} , I_{sc} , and FF of the device were 0.75 V, 3.8 mA/cm², and 56%, respectively, which indicates that BDT is a promising common unit for photovoltaic conjugated polymers. Since we have developed the synthetic method of the 4,8-bisalkoxy-BDT monomer, the BDT unit will play an important role in future research on conjugated polymer design.

Introduction

Conjugated polymers have attracted considerable attention due to their versatile applications in the fields of conducting polymers and conjugated polymer optoelectronic devices. As optoelectronic materials, conjugated polymers are broadly used in polymer light-emitting diodes (PLEDs),¹ polymer field effect transistors (PFETs),² sensors,³ photodetectors,⁴ polymer photovoltaic cells (PPVCs) or polymer solar cells (PSCs), etc.⁵ In order to get efficient electronic devices, it is necessary to tune their properties, such as band gap, molecular energy level, solubility, luminescence, absorbance and so on.⁶

For conjugated polymers used in PSC devices, bandgap and molecular energy levels are of crucial importance for device performance. The mismatch between absorption spectra of conjugated polymers and the solar irradiance spectrum is one of the main reasons for low efficiency of PSC devices. As shown in Figure 1, the spectrum of photon flux of sunlight exhibits a broadband in the range from 350 to 3000 nm with a peak at about 680 nm. However, the active layer of PSC devices can absorb only a small portion of sunlight. In fact, the absorption spectrum of poly(3-hexylthiophene) (P3HT), a widely used photovoltaic material, only covers the range of 300–650 nm.⁷ In order to improve light harvesting by PSCs, some small-bandgap polymers were introduced into PSCs.⁸ For example, poly[2,6-(4,4-bis(2-ethylhexyl)-4*H*-cyclopenta[2,1-*b*:3,4-*b'*] dithiophene)-*alt*-4,7-(2,1,3-benzothiadiazole)] (PCPDTBT) provides a better overlap with the solar spectrum than P3HT and was successfully used

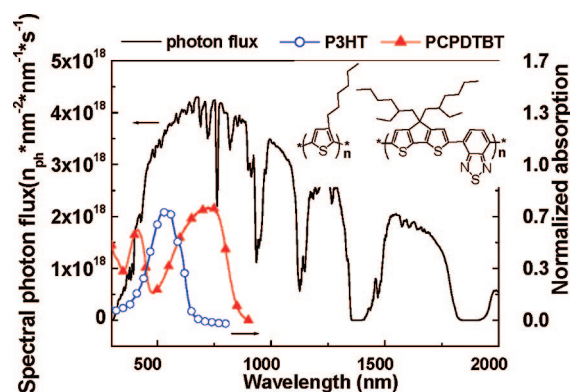
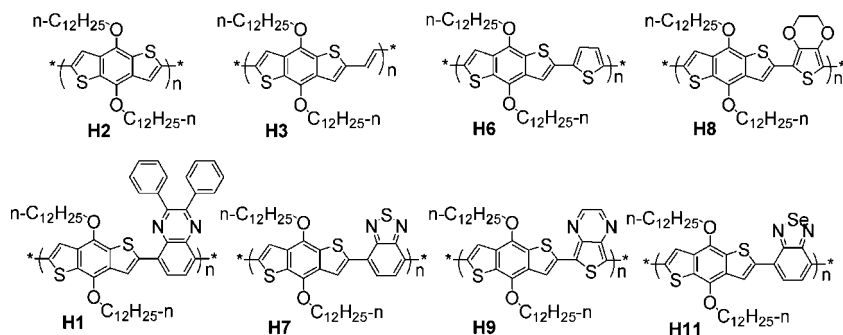


Figure 1. Solar photon flux (the solid line) spectra (AM1.5)¹⁴ and absorption spectra of two typical electron donor materials, poly(3-hexylthiophene) (the line with circles) and poly(2,6-diyl-4,4-bis(2-ethylhexyl)cyclopenta[2,1-*b*:3,4-*b'*]dithiophene)-*co*-(4,7-diylbenzo[1,2,5]thiadiazole) (the line with triangles).

in application of PSC.⁹ However, the molecular energy levels of the materials were not ideal yet, in that a great deal of energy of absorbed photons was lost during the photon–electron conversion process, which is another important reason for low efficiency of PSC devices. As shown in Figure 1, the energy of photons absorbed by active layer materials is more than 1.5 eV, but V_{oc} of the devices is only around 0.6 V. For PCPDTBT-based solar cells, more than 60% of the energy of absorbed photons is lost during the photon–electron conversion process; for P3HT-based solar cells, this kind of energy loss can get to more than 75%. As reported, V_{oc} of bulk heterojunction polymer solar cell varies directly with the gap between the lowest

* Corresponding authors. E-mail: jhhou@ucla.edu (J.H.); yangy@ucla.edu (Y.Y.).

Scheme 1. Structure of BDT-Based Polymers



unoccupied molecular orbit (LUMO) level of electron acceptor material and the highest occupied molecular orbit (HOMO) level of electron donor material.¹⁰ Therefore, to pursue higher V_{oc} , the electron donor material with a deeper HOMO level or electron acceptor material with a higher LUMO level should be employed in polymer solar cells.

HOMO and LUMO energy levels of conjugated polymers as well as their bandgaps are tunable by copolymerizing with different units. For example, the bandgap of poly(3-alkylthiophene) can be lowered from 1.85 to 1.55 eV after substituting with alkoxy groups at the 3-position. Correspondingly its HOMO level is elevated from -4.75 to -4.47 eV as a result of which V_{oc} of the PSC devices dropped from 0.6 V (for poly(3-alkylthiophene)-based device) to 0.02 V (for poly(3-alkoxythiophene)-based device).¹¹ The polymer of 4,4-dioctylcyclopenta[2,1-*b*:3,4-*b'*]dithiophene exhibited a bandgap of 1.8 eV and a HOMO level of -5.15 eV,¹² and after being copolymerized with 4,7-diylbenzo[*c*][1,2,5]thiadiazole, the band gap of the polymer was lowered to 1.4 eV, but its HOMO level had little change.^{9b,d} On the other hand, poly[5,7-bis(3-octylthiophen-2-yl)thieno{3,4-*b*}pyrazine] (PB3OTP), which is a copolymer of dithiophene and thieno[3,4-*b*]pyrazine (TPZ), has similar molecular structure and bandgap as PCPDTBT, but its HOMO level is much higher than that of PCPDTBT.¹³ Hence, V_{oc} of the PCPDTBT:PCBM solar cell device was 0.6 V, in comparison to 0.2 V for PB3OTP:PCBM solar cell devices. These results reveal that it is necessary to investigate effects of copolymerized functional units on bandgap and molecular energy levels of conjugated polymers. In this paper, effects of seven different but commonly used units on bandgap and molecular energy levels of conjugated polymers were investigated systematically, and these results provide some useful reference to control bandgap and molecular energy levels of conjugated polymers. Additionally, a family of conjugated polymer photovoltaic materials was designed, synthesized, and characterized systematically. Furthermore, the photovoltaic properties of the new polymers were also investigated by fabricating the PSC devices.

Design and Synthesis of the Polymers

BDT attracted some interest as a common unit in conjugated polymers,¹⁵ but some of the important properties of this unit have not been explored fully. In this paper, we designed and synthesized eight conjugated polymers based on BDT as shown in Scheme 1. There are two merits of choosing BDT as common unit of the polymers. First, BDT has a large planar conjugated structure and easily forms π - π stacking, which improves mobility. As reported, polymers based on BDT and thiophene exhibit a hole mobility of $0.25 \text{ cm}^2 \text{ V}^{-1} \text{ s}^{-1}$, one of the highest values for conjugated polymers.^{15b} So, it is reasonable to expect the BDT-based polymers to have good mobility. Second, since bandgap of conjugated polymers is generally very susceptible to steric hindrance, if we want to investigate the effects on

bandgap and molecular energy levels of different units, we must consider the steric hindrance between two adjacent units. For BDT, however, steric hindrance between adjacent units is very small, as 4,9-bis-alkoxy-BDT has no substituent on 1, 3, 5, and 7 positions. This makes BDT an ideal conjugated unit for new photovoltaic material design.

As shown in Scheme 1, 4,8-bis-dodecyloxy-BDT was copolymerized with seven different units including three kinds of electron-rich units and four electron-deficient units. The detailed synthesis routes are shown in Scheme 2. We further modified the method reported by Beimling et al. and improved the yield of the reactions.¹⁶ *N,N*-Diethylthiophene-3-carboxamide, compound **2**, was prepared from thiophene-3-carbonyl chloride and diethylamine with a yield more than 95%. Then, *N,N*-diethylthiophene-3-carboxamide was reacted with *n*-butyllithium in THF at 0 °C to produce the benzo[1,2-*b*:4,5-*b'*]dithiophene-4,8-dione, compound **3**, with a yield of 75%. Subsequently, compound **3** was reduced by zinc dust in aqueous sodium hydroxide solution. When the reduction reaction was complete, dodecyl bromide was added with a catalytic amount of tetrabutylammonium bromide. After being refluxed for 12 h, 4,8-bis(dodecyloxy)benzo[1,2-*b*:4,5-*b'*]dithiophene, compound **4**, was obtained with a yield of 78%, and then it was bromated as common method with a yield of 90%, giving 2,6-bis(trimethylstannyl)benzo[1,2-*b*:4,5-*b'*]dithiophene, compound **5**, with a yield of 80%. Then, polycondensation was carried out between organic tin compounds and bromides through the Stille coupling reaction.¹⁷

Thermal Stability

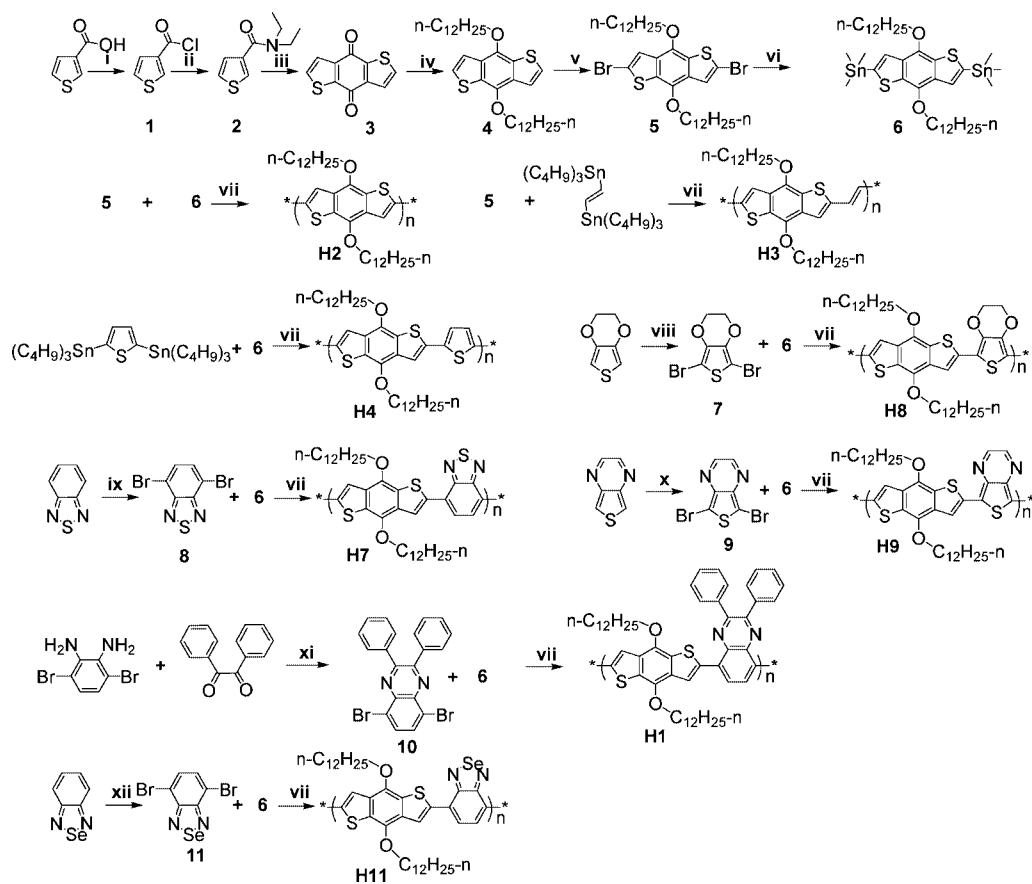
All of these BDT-based polymers exhibited very similar thermal stability, and Figure 2 shows the thermogravimetric analysis (TGA) plots of H6 and H7 as representative samples. The onset decomposition temperatures of the polymers are around 270 °C without protection of inert gas, due to leaving of alkoxy groups. Obviously, the thermal stability of the BDT-based polymers is adequate for their applications in PSCs and other optoelectronic devices.

Molecular Energy Level Measurements Using the Electrochemical Method

Electrochemical cyclic voltammetry (CV) was performed to determine the HOMO and the LUMO energy levels of the conjugated polymers.¹⁸ Figure 3 shows the cyclic voltammograms of the BDT-based polymer films on Pt electrode in 0.1 mol/L Bu_4NPF_6 , CH_3CN solution. From the value of onset oxidation potential (φ_{ox}) and onset reduction potential (φ_{red}) of the polymers, the HOMO and the LUMO as well as the bandgaps (E_g^{ec}) were calculated and listed in Table 1.

Absorption Spectra and Bandgap of the Polymers

The absorption spectra of the polymers in THF solution and in films are shown in Figures 4a and 3b. The three electron-

Scheme 2. Synthetic Routes of the Polymers^a

^a Conditions: (i) oxalyl chloride, methylene chloride, ambient temperature, overnight; (ii) diethylamine, methylene chloride, ambient temperature, 30 min; (iii) *n*-butyllithium, THF, ambient temperature, 30 min; then water, several hours; (iv) Zn, NaOH, H₂O, reflux for 1 h; then *n*-C₁₂H₂₅Br, TBAB, reflux for 6 h; (v) Br₂, methylene chloride, ambient temperature, 4–6 h; (vi) *n*-butyllithium, THF, –78 °C, 1 h, argon; then (CH₃)₃SnCl, ambient temperature, 2 h, argon; (vii) Pd(PPh₃)₄, toluene, 110 °C, 16 h, argon; (viii) NBS, DMF, 0 °C, then 2 h, ambient temperature; (ix) bromine, 48% hydrobromic acid, reflux for 6 h; (x) NBS, DMF, –10 °C, 30 min; then ambient temperature for 1 h; (xi) Chloroform, *p*-TSA, reflux for 12 h; (xii) bromine, Ag₂SO₄, 98% H₂SO₄, ambient temperature for 3 h.

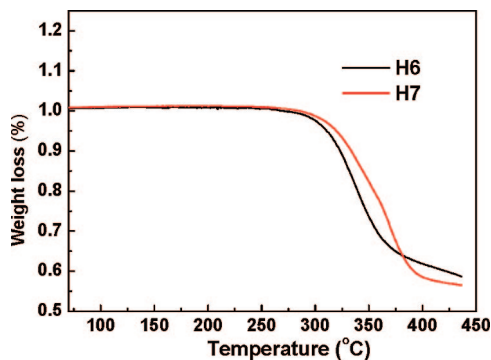


Figure 2. TGA plots of H6 and H7 with a heating rate of 10 °C/min under in the air.

rich units, ethylene, thiophene, and ethylenedioxythiophene (EDOT), affect bandgap of BDT polymer slightly. In films, the peak of absorption spectrum of the homopolymer of BDT, H2, is at about 495 nm. In comparison with H2, absorption spectra of H3 and H6 show a red shift by 10 nm, and the absorption spectrum of the polymer H8 shifts to the red direction by about 40 nm because of the strong electron-donating effect of EDOT. However, the four electron-deficient units exhibit a strong effect in lowering the bandgap of the BDT-based polymers. The order of bandgap-lowering ability of these four units was thieno[3,4-*b*]pyrazine (TPZ) >> benzo[*c*][1,2,5]selenadiazole (BSe) > 2,3-diphenylquinoxaline (DPQ) > benzo[*c*][1,2,5]thiadiazole (BT).

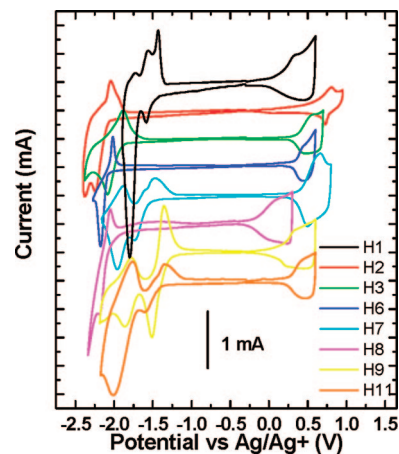


Figure 3. Cyclic voltammograms of the eight BDT-based polymers films on platinum electrode in 0.1 mol/L Bu₄NPF₆, CH₃CN solution.

Although TPZ and BT have the same molecular formula and similar structure, TPZ affects the absorption spectrum of the BDT-based polymer much more distinctly than BT. As shown in Figure 4, the absorption spectrum of H7 exhibits a peak at 591 nm and an absorption edge at 730 nm corresponding to a bandgap of 1.7 eV. In comparison with H7, the absorption spectrum of H9 shifts toward a longer wavelength by about 240 nm. The main reason for the difference between their absorption

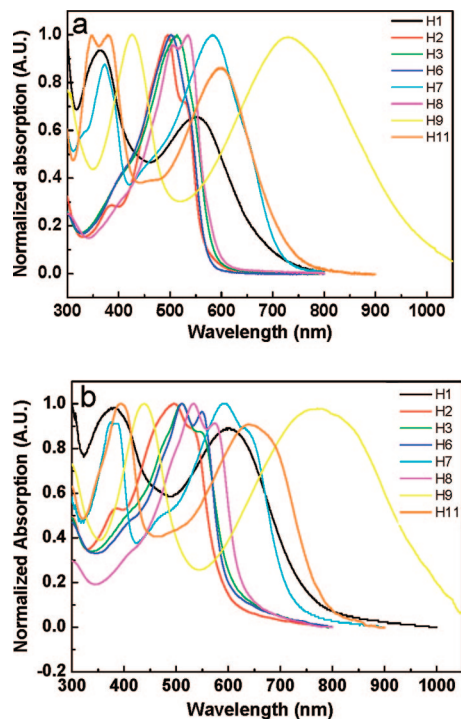
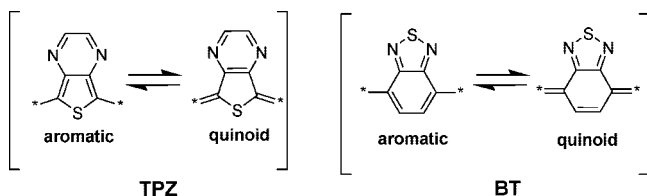


Figure 4. UV-vis absorption spectra of the polymers: (a) in THF solution (the absorption of H2 was measured using chloroform as solvent); (b) in films.

Scheme 3. Aromatic and Quinoid Forms of TPZ and BT Units



spectra is attributed to the different stabilities of their electron quinoid forms. Both TPZ and BT are fused aromatic heterocyclic compounds constituted of a six-member ring and a five-member ring. However, as shown in Scheme 3, TPZ is linked with adjacent aromatic units at the 5 and 7 positions on the five-member ring, but BT is linked with adjacent aromatic units at the 4 and 7 positions on the six-member ring. In the quinoid structure of TPZ, the six-member ring can form a more stable aromatic electron structure, whereas the electron structure of the five-member ring of BT has no change in its aromatic and quinoid structures. So, the six-member ring of TPZ will stabilize the quinoid structure better than the five-member ring of BT, and thus a more stable quinoid structure will be formed in polymer H9 than in H7. Since the quinoid form has a smaller bandgap than the aromatic form,¹⁹ the bandgap of H9 is lower than H7.

Photovoltaic Properties of the Polymers

Figure 5 shows the I - V curves of the PSC devices with champion performances under the illumination of AM1.5, 100 mW/cm², and Table 2 lists the photovoltaic properties obtained from the I - V curves. Polymer H2 exhibited good solubility in toluene and chlorobenzene above 80 °C but cannot be dissolved in cold solvent. So, a uniform film cannot be prepared for solar cell device, and photovoltaic properties of H2 are not presented in this paper.

As listed in Table 2, the photovoltaic properties of these materials are different from each other. For example, the power

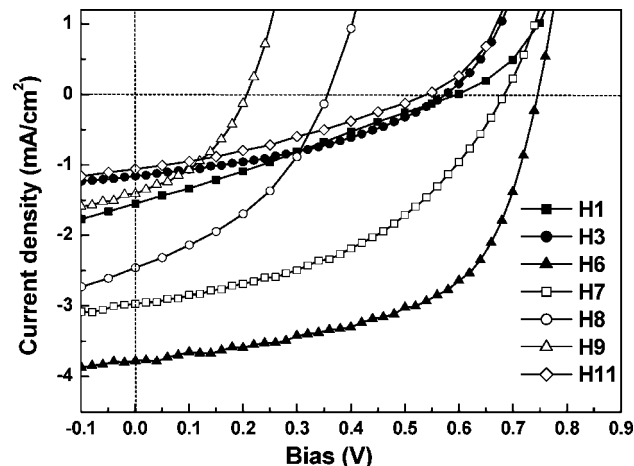


Figure 5. I - V curves of the polymer solar cells based on the new polymers under the illumination of AM 1.5, 100 mW/cm².

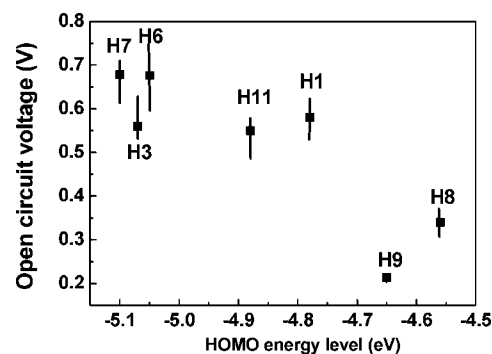


Figure 6. Open-circuit voltage distribution of the devices based on BDT polymers; average values are shown as squares.

conversion efficiency (PCE) of H6-based device is more than 10 times higher than that of H9. As known, the short circuit current (I_{sc}), fill factor (FF), and power conversion efficiency (PCE) are very susceptible to molecular structure of the polymers. For instance, the number of carbons in the alkyl side chain of polythiophene can greatly affect the hole mobility of poly(3-alkylthiophene)²⁰ as well as its photovoltaic properties,²¹ and under same conditions, the PCE of poly(3-hexylthiophene):PCBM-based device is about 10 times higher than that of poly(3-butylthiophene):PCBM-based device. Since the BDT-based polymers have identical side chains but different conjugated main chains, PCE, FF, and I_{sc} of devices based on them are not comparable.

In order to reveal the relationship between HOMO level of electron donor material and V_{oc} of the device, the variation of V_{oc} of the devices based on BDT polymers as a function of HOMO level is shown in Figure 6. It can be seen that, in general, V_{oc} of the devices varies inversely with HOMO level of the electron donor material. As listed in Table 1, the onset points of oxidation and reduction of H2 are 0.44 V (E_{ox}) and -2.05 V (E_{red}), corresponding to a HOMO level of -5.16 eV and a LUMO level of -2.67 eV. Polymer H8 has a similar E_{red} potential as H6, but E_{ox} of H8 is 0.49 V higher than that of H6, which is due to the strong electron-pushing effect of the 3,4-ethylenedioxythiophene units. As a result, V_{oc} of H6-based device was 0.38 V higher than the H8-based device, which indicates that insertion of electron-donating functional groups for lowering bandgap is not a feasible method in terms of photovoltaic properties of conjugated polymers. The four electron-deficient units also exhibited different effects on molecular energy levels of the BDT-based polymers. E_g of the polymer H9 reached 1.05 eV, which is the smallest among these

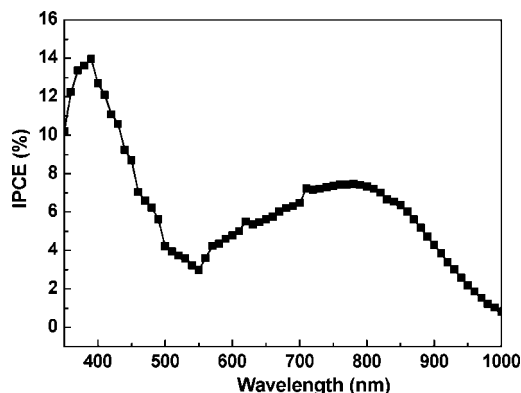


Figure 7. IPCE curve of the PSC device based on the polymer H9.

polymers, and its absorption spectrum matched the spectrum of solar irradiation very well. However, V_{oc} of the H9-based device is only 0.21 V because the HOMO level of H9 is too high. The BT unit has little influence on the HOMO level of the BDT-based polymer, and the HOMO of H7 is similar to that of H2. The LUMO level of H7 is lower than H2 by about 0.52 eV, which indicates that the BT unit can lower the bandgap by depressing the LUMO level only. As a result, V_{oc} of H7-based devices was 0.68 V, which is much higher than that of H9. The BSe unit, the analogue of BT, exhibited more effect on depressing the LUMO level of BDT-based polymer, but it also exhibited a small effect on elevating the HOMO level. The LUMO level of H11 is higher than H7 by 0.12 eV, and the LUMO level of H11 is lower than H7 by 0.14 eV. So, V_{oc} of the H11-based device was about 0.12 V lower than that of the H7-based device. Additionally, V_{oc} , I_{sc} , and FF of the PSC devices are susceptible to morphology of active layer, and some methods such as slow growth^{7a} and mixed solvent effect^{9a} influence morphology of active layer distinctly, and hence I_{sc} and FF of the devices can be improved greatly. We are working on investigating the relationship between morphology of active layers and performance of the BDT polymer-based devices and will report in the near future.

Since the polymer H9 exhibits a broad absorption spectrum extending to 1000 nm, we measured the input photon to converted current efficiency (IPCE) curve to investigate the response range of the material. As shown in Figure 7, the shape of the IPCE curve of the device based on H9 is very similar to its absorption spectrum, indicating that all the absorption of the polymer contributed to the photovoltaic conversion.

Conclusion

In this paper, eight BDT-based conjugated polymers (see Scheme 1) were designed and synthesized, and seven commonly used aromatic units were used to tailor the bandgap of the polymers as well as molecular energy levels. By copolymerizing with different units, bandgaps and molecular energy levels of the polymers can be tuned effectively. The effects of these units on bandgaps and molecular energy levels were investigated systematically by absorption spectroscopy and cyclic voltam-

metry methods. The PSC devices based on the polymers were fabricated and characterized. We found that the V_{oc} of the devices varied inversely with the HOMO level of the electron donor materials, and some units such as ethylenedioxythiophene and TPZ cannot be used as bandgap-lowering units in BDT polymers due to the fact that HOMO levels of the polymers were elevated too much after being copolymerized with these units. However, the BT unit can lower the bandgap by reducing the LUMO level only, and the BSe unit exhibits similar properties as BT. So, for optimization of bandgaps and molecular energy levels of BDT-based polymers, BT and BSe are preferable to TPZ and BPQ. These results provide some good reference to bandgap and molecular energy level control of BDT-based polymers and should also be useful for molecular structure design of other kinds of conjugated polymers serving in various electronic devices.

Although photovoltaic performance of the devices based on the new materials was lower than the device based on classic materials such as P3HT, the device based on H6:PCBM exhibited promising photovoltaic properties without any post-treatment. V_{oc} , I_{sc} , and FF of the H6-based device were 0.75 V, 3.8 mA/cm², and 56%, respectively, corresponding to a PCE of 1.6%, which indicates BDT is a promising common unit of photovoltaic conjugated polymers. Since we have developed the synthetic method of the 4,8-bisalkoxy-BDT monomer, the BDT unit will play an important role in future research on molecular structure design of conjugated polymer.

Experimental Section

Materials and Characterization. Tetrahydrofuran (THF) was dried over Na/benzophenone and freshly distilled prior to use. 2,5-Bis(tributylstannyl)thiophene,²² (*E*)-1,2-bis(tributylstannyl)ethane,²³ thieno[3,4-*b*]pyrazine,²⁴ and 5,8-dibromo-2,3-diphenylquinoxaline²⁵ were synthesized according to the methods reported in the literature. Other chemicals used in this work were commercial products and used as received.

¹H NMR and ¹³C NMR spectra were measured on a Bruker DMX-400 spectrometer. TGA measurement was performed on a TA Instruments 2050 TGA. Absorption spectra were taken using a Varian Cary 50 ultraviolet–visible spectrometer. The molecular weight of polymers was measured by the GPC method, and polystyrene was used as a standard. The electrochemical cyclic voltammetry was conducted with Pt disk coated with the polymer film, Pt wire, and Ag electrode as working electrode, counter electrode, and reference electrode, respectively, in a 0.1 mol/L tetrabutylammonium hexafluorophosphate (Bu₄NPF₆)–acetonitrile solution. Since Ag wire is a semireference electrode, a trace amount of ferrocene (Fc) was used as a standard material to determine the molecular energy level of the polymers. The thickness of the active layer of the polymer solar cell device was measured with a Dektak profilometer, and testing of the devices was done in a N₂-filled glovebox under AM 1.5G irradiation (100 mW cm⁻²) using a xenon lamp solar simulator calibrated with a silicon diode (with KG5 visible filter) calibrated with the assistance from the National Renewable Energy Laboratory (NREL). The spectral mismatch was corrected.

Fabrication of PSC Devices. PSC devices with the typical structure of ITO/PEDOT-PSS/polymer:PCBM(1:1, w/w)/Ca/Al were

Table 1. Optical Properties, Electrochemical Onset Potentials, and Electronic Energy Levels of the Polymers

	λ_{max} (nm)	E_g^{opt} (eV)	E_{ox} (V)	HOMO (eV)	E_{red} (V)	LUMO (eV)	E_g^{ec} (eV)
H1	601	1.63	0.06	-4.78	-1.44	-3.28	1.50
H2	495	2.13	0.44	-5.16	-2.05	-2.67	2.49
H3	510	2.03	0.35	-5.07	-1.86	-2.86	2.21
H6	511	2.06	0.33	-5.05	-2.07	-2.69	2.36
H7	591	1.70	0.38	-5.10	-1.53	-3.19	1.91
H8	532	1.97	-0.16	-4.56	-2.06	-2.66	1.90
H9	780	1.05	-0.07	-4.65	-1.26	-3.46	1.19
H11	641	1.52	0.26	-4.88	-1.39	-3.33	1.55

fabricated under similar conditions as follows: After spin-coating a 30 nm layer of poly(3,4-ethylenedioxythiophene):poly(styrenesulfonate) onto precleaned indium–tin oxide (ITO)-coated glass substrates, the polymer/PCBM blend solution was spin-coated. Typical concentration of the polymer/PCBM (1:1, w/w) blend solution used in this study for spin-coating active layer was 20 mg/mL, and chlorobenzene was used as solvent. The thickness of the active layer was ~100 nm, and no further treatment to the blend film was performed in this study. The devices were completed by evaporating Ca/Al metal electrodes with area of 10.5 mm² defined by masks. For H1-based devices, a 1 nm of thin LiF layer was used instead of Ca.

Synthesis of Materials. *Thiophene-3-carbonyl Chloride, 1.* Thiophene-3-carboxylic acid (38.4 g, 0.3 mol) and 60 mL of methylene chloride were put into a 250 mL flask. The mixture was cooled by ice–water bath, and then oxalyl chloride (76.2 g, 0.6 mol) was added in one portion. The reactant was stirred overnight at ambient temperature, and a clear solution was obtained. After removing the solvent and unreacted oxalyl chloride by rotary evaporation, compound **1** was obtained as colorless solid. It was dissolved into 100 mL of methylene chloride and used for the next step.

N,N-Diethylthiophene-3-carboxamide, 2. In a 500 mL flask in ice–water bath, 62.5 mL of diethylamine (43.8 g, 0.6 mol) and 100 mL of methylene chloride were mixed, and the solution of thiophene-3-carbonyl chloride was added into the flask slowly. After all of the solution was added, the ice bath was removed, and the reactant was stirred at ambient temperature for 30 min. Then, the reactant was washed by water several times, and the organic layer was dried over anhydrous MgSO₄. After removing solvent, the crude product was purified by distillation under vacuum, and 49 g of compound **2** (0.27 mol, yield 90%) was obtained as a pale yellow oil. GC-MS: *m/z* = 183. ¹H NMR (CDCl₃, 400 MHz), δ (ppm): 7.48 (s, 1H), 7.32 (d, 1H), 7.20 (d, 1H), 3.41 (m, 4H), 1.19 (t, 6H).

4,8-Dihydrobenzo[1,2-b:4,5-b']dithiophene-4,8-dione, 3. Compound **2** (0.2 mol, 36.6 g) was put into a well-dried flask with 200 mL of THF under an inert atmosphere. The solution was cooled down by an ice–water bath, and 70 mL of *n*-butyllithium (0.2 mol, 2.9 mol/L) was added into the flask dropwise within 30 min. Then, the reactant was stirred at ambient temperature for 30 min. The reactant was poured into 500 g of ice water and stirred for several hours. The mixture was filtrated, and the yellow precipitate was washed by 200 mL of water, 50 mL of methanol, and 50 mL of hexane successively. 34.3 g of compound **3** was obtained as a yellow powder (0.16 mol, yield 78%). GC-MS: *m/z* = 220. IR (KBr): 1640 cm⁻¹ (C=O). ¹H NMR (CDCl₃, 400 MHz), δ (ppm): 7.75 (d, 2H), 7.95 (d, 2H).

4,8-Didodecyloxybenzo[1,2-b:3,4-b']dithiophene, 4. Compound **3** (4.4 g, 20 mmol), zinc powder (2.86 g, 44 mmol), and 60 mL of water were put into a 250 mL flask; then 12 g of NaOH was added into the mixture. The mixture was well stirred and heated to reflux for 1 h. During the reaction, the color of the mixture changed from yellow to red and then to orange. Then, 1-bromododecane (15 g, 60 mmol) and a catalytic amount of tetrabutylammonium bromide were added into the flask. After being refluxed for 2 h, the color of the reactant should be yellow or orange; if the color of the reactant was red or deep red, an excess amount of zinc powder (1.3 g, 20 mmol) should be added. Then, the reactant was refluxed for 6 h. The reactant was poured into cold water and extracted by 200 mL of diethyl ether two times. The ether layer was dried over anhydrous MgSO₄. After removing solvent, the crude product was purified by recrystallization from ethyl alcohol two times. 9.26 g of compound **4** (16.6 mmol, yield 83) was obtained as colorless crystal. ¹H NMR (CDCl₃, 400 MHz), δ (ppm): 7.66 (d, 2H), 7.47 (d, 2H), 4.26 (t, 4H), 1.87 (quintuple, 4H), 1.53 (m, 4H), 1.37–1.27 (m, 32H), 0.88 (t, 6H). Elemental analysis: Calculated for C₃₄H₅₄O₂S₂: C, 73.06; H, 9.74. Found: C, 72.89; H, 9.70.

2,6-Dibromo-4,8-didodecyloxybenzo[1,2-b:3,4-b']dithiophene, 5. Compound **4** (5.58 g, 10 mmol) was dissolved into 100 mL of methylene chloride in a 250 mL flask. Bromine (3.2 g, 20 mmol) was dissolved into 60 mL of methylene chloride in a funnel and slowly dropped into the flask under an ice–water bath, and then the reactant was stirred for 4–6 h at ambient temperature. When color of bromine was diminished, all volatile substances were removed under vacuum.

Table 2. Photovoltaic Properties of the Polymer Solar Cells

	V _{oc} (V)	I _{sc} (mA/cm ²)	FF (%)	PCE (%)
H1	0.60	1.54	26	0.23
H3	0.56	1.16	38	0.25
H6	0.75	3.78	56	1.60
H7	0.68	2.97	44	0.90
H8	0.37	2.46	40	0.36
H9	0.22	1.41	35	0.11
H11	0.55	1.05	32	0.18

Table 3. Molecular Weight and Elemental Analysis Data of the Polymers

	yield (%)	molecular weight data		elemental analysis data		
		M _n	PDI	C	H	N
H1	67	20.2K	2.0	73.98	8.09	3.54
H2	78			74.01	9.51	
H3	54	67.1K	2.2	73.84	9.81	
H6	34	46.7K	1.8	71.22	8.75	
H7	67	18.5K	1.7	69.78	7.78	3.97
H8	46	29.1K	1.9	68.13	8.34	
H9	51	34.6K	2.2	69.71	7.97	4.01
H11	37	16.9K	2.1	65.65	7.56	3.89

The residue was recrystallized by hexane one time. 6.37 g of compound **5** (8.9 mmol, yield 89%) was obtained as a white solid. ¹H NMR (CDCl₃, 400 MHz), δ (ppm): 7.43 (s, 2H), 4.17 (t, 4H), 1.83 (quintuple, 4H), 1.54 (m, 4H), 1.36–1.27 (m, 32H), 0.89 (t, 6H). Elemental analysis: Calculated for C₃₄H₅₂Br₂O₂S₂: C, 56.98; H, 7.31. Found: C, 56.78; H, 7.39.

2,6-Bis(trimethyltin)-4,8-didodecyloxybenzo[1,2-b:3,4-b']dithiophene, 6. Compound **5** (4.30 g, 6 mmol) and 100 mL of THF were added into a flask under an inert atmosphere. The solution was cooled down to –78 °C by a liquid nitrogen–acetone bath, and 4.55 mL of *n*-butyllithium (13.2 mmol, 2.9 M in *n*-hexane) was added dropwise. After being stirred at –78 °C for 1 h, a great deal of white solid precipitate appeared in the flask. Then, 14 mmol of trimethyltin chloride (14 mL, 1 M in *n*-hexane) was added in one portion, and the reactant turned to clear rapidly. The cooling bath was removed, and the reactant was stirred at ambient temperature for 2 h. Then, it was poured into 200 mL of cool water and extracted by ether three times. The organic layer was washed by water two times and then dried by anhydrous MgSO₄. After removing solvent under vacuum, the residue was recrystallized by ethyl alcohol two times. 4.03 g of compound **6** (4.56 mmol, yield 76%) was obtained as colorless needle crystal. ¹H NMR (CDCl₃, 400 MHz), δ (ppm): 7.63 (s, 2H), 4.17 (t, 4H), 1.86 (quintuple, 4H), 1.54 (m, 4H), 1.35–1.27 (m, 32H), 0.87 (t, 6H). ¹³C NMR (CDCl₃, 100 MHz), δ (ppm): 143.131, 140.488, 134.046, 133.009, 129.105, 128.042, 73.618, 31.958, 30.576, 29.736, 29.697, 29.537, 29.402, 26.157, 22.724, 14.154, –8.298. Elemental analysis: Calculated for C₄₀H₇₀O₂S₂Sn₂: C, 54.31; H, 7.98. Found: C, 54.13; H, 7.78.

2,5-Dibromo-3,4-ethylenedioxythiophene, 7. In a 250 mL flask, 3,4-ethylenedioxythiophene (1.42 g, 10 mmol) was dissolved into 30 mL of DMF, and the flask was cooled down to 0 °C by an ice–water bath. In a funnel, *N,N'*-bromosuccinimide (3.78 g, 21 mmol) was dissolved into 30 mL of DMF, and then this solution was dropped into the flask slowly. When all of the solution was added, the cool bath was removed, and the reactant was stirred for 2 h at ambient temperature to complete the bromination reaction. Then, 100 mL of cold water was added into the flask slowly, and a great deal of compound **7** was precipitated as white or pale yellow solid. The precipitate was collected by filter under vacuum and washed by water several times. By GC-MS, we found that purity of the product was more than 98%, which was good enough for polymerization without further purification. The yield of the reaction was close to 100%. GC-MS: *m/z* = 498. IR (KBr, ν cm⁻¹): 459, 951, 1080, 1357, 1413, 1504, 2873, 2947. ¹H NMR (CDCl₃, 400 MHz), δ (ppm): 4.13 (s). ¹³C NMR (CDCl₃, 100 MHz), δ (ppm): 139.3, 85.1, 64.6.

4,7-Dibromo-2,1,3-benzothiadiazole, 8. 2,1,3-Benzothiadiazole (5.0 g, 36.8 mmol) of was put into a 250 mL two-necked flask with 75 mL of 48% hydrobromic acid, and the mixture was heated to reflux.

A solution containing Br₂ (17.6 g, 110 mmol) in 50 mL of hydrobromic acid was added dropwise very slowly. After completion of the bromine addition, the reaction mixture was fluxed for 6 h, and a great deal of needle crystals was precipitated. Then, the mixture was cooled down to room temperature, then filtered, and washed by water several times, and then the solid was recrystallized by chloroform. Compound **8** was obtained as pale yellow needle crystals (9.7 g, yield 90%). GC-MS: *m/z* = 292. ¹H NMR (CDCl₃, 400 MHz), δ (ppm): 7.74 (s, 2H). ¹³C NMR (CDCl₃, 100 MHz), δ (ppm): 154.01, 132.34, 113, 98.

5,7-Dibromothieno[3,4-*b*]pyrazine, 9. Thieno[3,4-*b*]pyrazine (1.36 g, 10 mmol) was dissolved in 30 mL of DMF, and the solution was cooled down to -10 °C. Then, 3.56 g of NBS was added into the flask in small portions. The reactant was stirred at -10 °C for 30 min, and the cool bath was removed. After being stirred at ambient temperature for 1 h, the reactant was poured into 100 mL of cold water and extracted by ethyl ether three times. The organic layer was washed by water and then dried by anhydrous MgSO₄. After removing solvent under vacuum, purification was carried out via silica gel column chromatography, using methylene chloride as the eluent. After removing of solvent, 1.58 g (54 mmol, yield 54%) of compound **9** was obtained as tan crystals. GC-MS: *m/z* = 292. ¹H NMR (CDCl₃, 400 MHz), δ (ppm): 7.83 (s, 2H).

5,8-Dibromo-2,3-diphenylquinoxaline, 10.²⁶ 3,6-Dibromobenzene-1,2-diamine (1.32 g, 5 mmol) was dissolved into 100 mL of chloroform, and then diphenylethanedione (1.05 g, 5 mmol) and catalytic *p*-TSA were added. The solution was stirred under for 12 h. Then, saturated aqueous NaHCO₃ (50 mL) was added to quench the reaction, and the mixture was extracted with methylene chloride. The combined organic layers were dried over anhydrous MgSO₄, filtered, and evaporated. The residue was purified by column chromatography on silica gel, using methylene chloride as the eluent. The title compound was obtained as pale yellow needle crystals (1.22 g, yield 56%). GC-MS: *m/z* = 438. ¹H NMR (CDCl₃, 400 MHz), δ (ppm): δ 7.92 (s, 2H), 7.67 (d, 4H), 7.42–7.33 (m, 6H). ¹³C NMR (CDCl₃, 100 MHz), δ (ppm): δ 154.11, 139.32, 137.82, 133.15, 130.31, 129.59, 128.24, 123.89.

4,7-Dibromobenzo[*c*][1,2,5]selenadiazole, 11. In a 100 mL flask, benzo[*c*][1,2,5]selenadiazole (1.83 g, 10 mmol) and silver sulfate (3.12 g, 10 mmol) were suspended into 25 mL of concentrated sulfuric acid and stirred for several minutes. Then, bromine (3.52 g, 22 mmol) was added into the flask dropwise, and the reactant was stirred at ambient temperature for 3 h and filtered. The flask and the precipitate were washed by 20 mL of concentrated sulfuric acid. The filtrate was added into 200 mL of ice–water slowly, and the crude product was precipitated as yellow solid, collected by filtration, and washed by water several times. After being purified by recrystallization with ethyl acetate, the title compound was obtained as yellow solid (1.47 g, yield 43%). GC-MS: *m/z* = 340. ¹H NMR (CDCl₃, 400 MHz), δ (ppm): 7.64 (s, 2H). ¹³C NMR (CDCl₃): 157.2, 132.1, 116.5.

Synthesis of the Polymers Using Stille Coupling Reaction. These six polymers were prepared with the same procedure as coupling dibromide compounds with bis(tributylstannyl)-substituted compounds.

1.0 mmol of dibromide compound, 1.0 mmol of bis(tributylstannyl)-substituted compound, and 50 mL of toluene were put into a two-necked flask with oil bath. The solution was flushed with argon for 10 min, and then 20 mg of Pd(PPh₃)₄ was added into the flask. The solution was flushed again for 20 min. The oil bath was heated to 110 °C carefully, and the reactant was stirred for 16 h at this temperature under an argon atmosphere. Then, the reactant was cooled to room temperature, and the polymer was precipitated by addition of 100 mL of methanol and filtered through a Soxhlet thimble, which was then subjected to Soxhlet extraction with methanol, hexane, and chloroform. The polymer was recovered as a solid sample from the chloroform fraction by rotary evaporation. The solid was dried under vacuum for 1 day to get the final product. The yields of the polymerization reactions were about 40–60%.

Acknowledgment. This work was financially supported by Solarmer Energy Inc., UC Discovery Grant (Grant GCP05-10208).

References and Notes

- (1) (a) Burroughes, J. H.; Bradley, D. D. C.; Brown, A. B.; Marks, R. N.; Mackay, K.; Friend, R. H.; Burn, P. L.; Holmes, A. B. *Nature (London)* **1990**, *347*, 539. (b) Hide, F.; Diaz-Garcia, M. A.; Schwartz, B. J.; Heeger, A. J. *Acc. Chem. Res.* **1997**, *30*, 430. (c) Friend, R. H.; Gymer, R. W.; Holmes, A. B.; Burroughes, J. H.; Marks, R. N.; Taliani, C.; Bradley, D. D. C.; Dos Santos, D. A.; Brédas, J. L.; Lögdlund, M.; Salaneck, W. R. *Nature (London)* **1999**, *397*, 121. (d) Gross, M.; Müller, D. C.; Nothofer, H.-G.; Scherf, U.; Neher, D.; Bräuchle, C.; Meerholz, K. *Nature (London)* **2000**, *405*, 661. (e) Müller, D. C.; Falcou, A.; Reckefuss, N.; Rohahn, M.; Wloderhirm, V.; Rudati, P.; Frohne, H.; Nuyken, O.; Becker, H.; Meerhotz, K. *Nature (London)* **2003**, *421*, 829.
- (2) (a) Sirringhaus, H.; Tessler, N.; Friend, R. H. *Science* **1998**, *280*, 1741. (b) Svensson, M.; Zhang, F. L.; Veenstra, S. C.; Verhees, W. J. H.; Hummelen, J. C.; Kroon, J. M.; Inganäs, O.; Andersson, M. R. *Adv. Mater.* **2003**, *15*, 988. (c) Coakley, K. M.; McGehee, M. D. *Chem. Mater.* **2004**, *16*, 4533.
- (3) Chen, L.; McBranch, D. W.; Wang, H.; Helgeson, R.; Wudl, F.; Whitten, D. G. *Proc. Natl. Acad. Sci. U.S.A.* **1999**, *96*, 12287.
- (4) Yu, G.; Wang, J.; McElvain, J.; Heeger, A. J. *Adv. Mater.* **1998**, *10*, 1431.
- (5) (a) Skotheim, T. A.; Elsenbaumer, R. L.; Reynolds, J. R., Eds.; *Handbook of Conducting Polymers*, 2nd ed.; Marcel Dekker: New York, 1998; Chapters 32–38. (b) Brabec, C. J.; Dyakonov, V.; Parisi, J.; Sariciftci, N. S. *Organic Photovoltaics: Concepts and Realization*; Springer-Verlag: Heidelberg, 2003. (c) Skotheim, T. A.; Reynolds, J. *Conjugated Polymers: Processing and Applications*; Taylor and Francis: Oxford, 2006.
- (6) (a) Roncali, J. *Chem. Rev.* **1997**, *97*, 173. (b) Meyers, F.; Heeger, A. J.; Brédas, J. L. *J. Chem. Phys.* **1992**, *97*, 2750.
- (7) (a) Li, G.; Shrotriya, V.; Huang, J.; Yao, Y.; Moriarty, T.; Emery, K.; Yang, Y. *Nat. Mater.* **2005**, *4*, 865. (b) Hou, J.; Tan, Z.; Yan, Y.; He, Y.; Yang, C.; Li, Y. *J. Am. Chem. Soc.* **2006**, *128*, 4911.
- (8) Winder, C.; Sariciftci, N. S. *J. Mater. Chem.* **2004**, *14*, 1077.
- (9) (a) Peet, J.; Kim, J. Y.; Coates, N. E.; Ma, W. L.; Moses, D.; Heeger, A. J.; Bazan, G. C. *Nat. Mater.* **2007**, *6*, 497. (b) Mühlbacher, D.; Scharber, M.; Morana, M.; Zhu, Z.; Waller, D.; Gaudiana, R.; Brabec, C. *Adv. Mater.* **2006**, *18*, 2884. (c) Soci, C.; Hwang, I.; Moses, D.; Zhu, Z.; Waller, D.; Gaudiana, R.; Brabec, C. J.; Heeger, A. J. *Adv. Funct. Mater.* **2007**, *17*, 632. (d) Zhu, Z.; Waller, D.; Gaudiana, R.; Morana, M.; Mühlbacher, D.; Scharber, M.; Brabec, C. *Macromolecules* **2007**, *40*, 1981.
- (10) Scharber, M. C.; Mühlbacher, D.; Koppe, M.; Denk, P.; Waldauf, C.; Heeger, A. J.; Brabec, C. J. *Adv. Mater.* **2006**, *18*, 789.
- (11) Shi, C.; Yao, Y.; Yang, Y.; Pei, Q. *J. Am. Chem. Soc.* **2006**, *128*, 8980.
- (12) (a) Wu, C.; Lu, M.; Chang, S.; Wei, C. *Adv. Funct. Mater.* **2007**, *17*, 1063. (b) Coppo, P.; Cupertino, D. C.; Yeates, S. G.; Turner, M. L. *Macromolecules* **2003**, *36*, 2705.
- (13) Campos, L. M.; Tontcheva, A.; Gunes, S.; Sonmez, G.; Neugebauer, H.; Sariciftci, N. S.; Wudl, F. *Chem. Mater.* **2005**, *17*, 4031.
- (14) The data of Solar Spectral Irradiance (air mass 1.5) was obtained from the Web site <http://rredc.nrel.gov/solar/spectra/am1.5/>.
- (15) (a) Hiraishi, K.; Yamamoto, T. *Synth. Met.* **2002**, *130*, 139. (b) Pan, H.; Li, Y.; Wu, Y.; Liu, P.; Ong, B. S.; Zhu, S.; Xu, G. *J. Am. Chem. Soc.* **2007**, *129*, 4112.
- (16) Beimling, P.; Kossmehl, G. *Chem. Ber.* **1986**, *119*, 3198.
- (17) (a) Milstein, D.; Stille, J. K. *J. Am. Chem. Soc.* **1978**, *100*, 3636. (b) Hou, J.; Huo, L.; He, C.; Yang, C.; Li, Y. *Macromolecules* **2006**, *39*, 594.
- (18) (a) Li, Y. F.; Cao, Y.; Gao, J.; Wang, D. L.; Yu, G.; Heeger, A. J. *Synth. Met.* **1999**, *99*, 243. (b) Sun, Q. J.; Wang, H. Q.; Yang, C. H.; Li, Y. F. *J. Mater. Chem.* **2003**, *13*, 800.
- (19) Brédas, J. L. *J. Chem. Phys.* **1985**, *82*, 3808.
- (20) Kaneto, K.; Lim, W. Y.; Takashima, W.; Endo, T.; Rikukawa, M. *Jpn. J. Appl. Phys.* **2000**, *39*, L872.
- (21) Nguyen, L. H.; Hoppe, H.; Erb, T.; Günes, S.; Gobsch, G.; Sariciftci, N. S. *Adv. Funct. Mater.* **2007**, *17*, 1071.
- (22) Hou, J.; Huo, L.; He, C.; Yang, C.; Li, Y. *Macromolecules* **2006**, *39*, 594.
- (23) Hou, J.; Tan, Z.; He, Y.; Yang, C.; Li, Y. *Macromolecules* **2006**, *39*, 4657.
- (24) Kenning, D. D.; Mitchell, K. A.; Calhoun, T. R.; Funfar, M. R.; Sattler, D. J.; Rasmussen, S. C. *J. Org. Chem.* **2002**, *67*, 9073.
- (25) Yamamoto, T.; Sugiyama, K.; Kushida, T.; Inoue, T.; Kanbara, T. *J. Am. Chem. Soc.* **1996**, *118*, 3930.
- (26) Chen, C.-T.; Wei, Y.; Lin, J.-S.; Moturu, M. V. R. K.; Chao, W.-S.; Tao, Y.-T.; Chien, C.-H. *J. Am. Chem. Soc.* **2006**, *128*, 10992.

MA800820R